ASSESSMENT OF COMBUSTION EFFICIENCIES OF EXISTING BOILERS AND THEIR IMPACTS ON CAMPUS AIR QUALITY (CO AND NO_2) THROUGH AIR QUALITY DISPERSION MODELING: THE CASE OF BİLECİK, TÜRKİYE

Edip Avşar[1], Seher SARI[2], Faruk ÜNLÜ[3], Veli ARSLAN[3]

[1]Professor, Bilecik Şeyh Edebali University Bilecik/Türkiye

[2]Lecturer, Eskişehir Technical University Eskişehir/Türkiye

[3]Engineer, Bilecik Şeyh Edebali University Bilecik/Türkiye

This work has been supported by Bilecik Şeyh Edebali University Scientific Research Projects Coordination Unit under grant number "2022-02.BŞEÜ.11-02"

ABSTRACT

Air pollution is one of the most important environmental problems in cities. Today, industrial activities are the most important source of air pollution. In addition, burning fuel due to heating increases air pollution problems and makes life in cities more difficult. Fossil fuels are used extensively for heating purposes. The low quality of these fuels (moisture, ash, sulfur content) as well as inefficiencies in combustion systems directly affect air pollution events and increase pollution to significant levels. Fossil fuels (natural gas) are also used for heating purposes in our campus. In addition to the quality of these fuels, the determination of the efficiency levels of the combustion systems in which the fuels are burned is also extremely important in preventing air pollution events. In inefficient systems, both the amount of fuel used and the emissions after combustion increase. The aim of the study is to determine and evaluate the effects of heating-related activities carried out in the central campus of our university on campus air quality. The aim of the study is to determine and evaluate the effects of heating-related activities carried out in the central campus of our university on the campus air quality. In this context, measurements were carried out to determine the combustion efficiency of a total of 6 boilers on our campus. The data obtained from the measurements were put into the distribution model through the air quality modeling program and the contribution to the air quality on the campus was revealed. In general, it is seen that the pollution values are well below the limit values and the maximum concentrations are detected in the southwest of the campus with the movement of the wind.

Keywords: Aermod, Air quality, Campus, Modelling

INTRODUCTION

When national and international studies on air quality in university campuses are examined, it is evident that pollution sources are primarily associated with traffic, geographical characteristics, meteorological conditions, and environmental heating systems.

At Bursa Uludağ University, Türkiye, air quality measurements conducted between 2013 and 2018 indicated that no sulfur dioxide (SO_2) pollution was detected on campus. Although annual exceedances of fine particulate matter ($PM_{2.5}$) were not severe, seasonal increases during winter months negatively affected air quality. Regarding nitrogen dioxide (NO_2), exceedances of regulatory threshold values were reported, particularly during the September-March period, mainly after 2017, due to both vehicle emissions and natural gas consumption (Url, 1).

A study conducted at the University of Bucharest, Romania, investigating traffic-related emissions on campus revealed that pollution levels varied according to weather conditions. On a sunny day with normal traffic flow, benzene concentrations exceeded the regulatory limit (5.4 $\mu g/m^3$), whereas on rainy days, the accumulation of harmful volatile organic compounds (VOCs), including benzene, toluene, ethylbenzene, and xylene (BTEX), was significantly reduced due to atmospheric washout processes (Popescu & Popescu, 2017).

Research carried out at Wuhan University, China, demonstrated that a substantial proportion of particulate matter (PM) pollution on campus originated from emissions produced by vehicles traveling on the adjacent main roadway. Furthermore, hourly fluctuations in emissions were found to be directly correlated with traffic volume (Liu et al., 2020).

At Tsinghua University, China, a health behavior study involving 12,000 students investigated the effects of $PM_{2.5}$ exposure. The findings indicated that increasing $PM_{2.5}$ concentrations negatively affected students' walking activities, vigorous physical exercise, and sedentary behavior duration, while positively influencing both daytime and nighttime sleep duration (An & Yu, 2018).

At Eskişehir Technical University, Türkiye, simultaneous measurements conducted during the COVID-19 lockdown period showed that indoor-to-outdoor (I/O) ratios for SO_2, NO_2, O_3, bacteria, and fungi were all below unity (<1). This finding suggests that outdoor pollutant concentrations exceeded those measured indoors (Bhat et al., 2022).

A study conducted at Ahmedabad College, India, reported that although campus air quality was cleaner than that of the surrounding urban environment, pollutant concentrations still exceeded recommended standards. Due to limited atmospheric dispersion, PM_{10} (173.02 $\mu g/m^3$) and $PM_{2.5}$ (75.74 $\mu g/m^3$) levels reached nearly twice the legal limits. In addition, significant fluctuations in black carbon concentrations were observed during evening hours (Daxini, 2020).

Research conducted at Białystok University of Technology, Poland, revealed that $PM_{2.5}$ and PM_{10} concentrations reached their highest levels during morning and evening hours. Increasing ambient temperatures were associated with reduced particulate matter concentrations, whereas low wind speeds facilitated exceedances of regulatory limits (Szatyłowicz, 2023).

A study carried out at Lodz University of Technology, Poland, demonstrated that pollutant dispersion mechanisms within densely built urban environments are highly complex. Distinct accumulation zones were observed depending on wind direction, and the primary sources contributing to campus air pollution were identified as nearby industrial facilities and the heating systems of multi-story residential buildings (Cichowicz & Dobranski, 2022).

Studies on air pollution and its impacts in Türkiye began in the 1960s, primarily centered in Ankara, and gradually evolved to focus on specific respiratory health outcomes. Data from 2016-2019 indicated that particulate matter pollution did not substantially decline nationwide, that pollution became persistent in several provinces, and that some monitoring stations remained inadequate in terms of measurement capacity (Bostan & Olcay, 2022).

Based on the literature review, it is evident that most studies conducted at universities and colleges have primarily focused on indoor air quality. In contrast, investigations examining outdoor air pollution within university campuses remain limited, highlighting the innovative and original contribution of future research in this area.

As of 2022, Bilecik Şeyh Edebali University (BSEU) ranked 275th worldwide and 15th nationally in the UI GreenMetric World University Rankings, thereby becoming part of the global green campus network. The primary objective of this network is to promote environmentally sustainable practices, conserve resources, increase the use of renewable energy, and reduce institutional carbon and water footprints. One of the key strategies supporting these objectives, and the focus of the present study, involves improving the efficiency of campus heating boilers in order to decrease fuel consumption associated with heating activities and reduce combustion-related atmospheric emissions, thereby enhancing campus air quality.

Accordingly, this study assessed the impact of heating-related activities on air quality within the central campus of Bilecik Şeyh Edebali University. Measurements were conducted to determine the combustion efficiency of six existing heating boilers located on campus. The data obtained were subsequently incorporated into the AERMOD air quality dispersion modeling software, and the contribution of heating-related emissions to campus air quality was simulated and evaluated with respect to carbon monoxide (CO) and nitrogen dioxide (NO_2) concentrations.

Recent studies have examined the atmospheric distribution of major outdoor air pollutants such as carbon monoxide (CO) and nitrogen dioxide (NO_2), variability in emission sources, and the neurological, respiratory, and metabolic health outcomes associated with exposure to these pollutants in a comprehensive manner (D'Amico et al., 2025; Park et al., 2025; Chen et al., 2025; Sun et al., 2025; Aljafen et al., 2025). Analyses of concentration dynamics indicate that gaseous pollution exhibits substantial fluctuations in response to both anthropogenic activities and meteorological conditions. For instance, a study conducted at a coastal monitoring station in Southern Italy demonstrated that the ozone-to-nitrogen oxide ratio (O_3/NO_x) could be utilized as an indicator of air mass aging, thereby allowing regional emission sources of CO and NO_2 to be identified more effectively (D'Amico et al., 2025). The study further reported that local anthropogenic emissions, particularly those associated with heavy traffic, residential heating systems during winter months, and wildfires during summer periods, generated pronounced seasonal and diurnal peaks in ambient CO and NO_x concentrations (D'Amico et al., 2025). The impacts of outdoor air pollution are not confined to open environments; a study conducted in Canada demonstrated that increases in outdoor NO_2 concentrations directly elevated indoor NO_2 levels through ventilation-related activities such as window opening, highlighting the penetration of outdoor pollution into indoor environments (Sun et al., 2025).

Among the most significant health consequences of air pollution are respiratory diseases. Outdoor CO and NO_2 concentrations are widely recognized as principal indicators of traffic-related air pollution

and have been strongly associated with the risk of developing Chronic Obstructive Pulmonary Disease (COPD) (Park et al., 2025). In a large multiethnic cohort study conducted in California, every 20 ppb increase in ambient NO_2 concentration and every 1000 ppb increase in CO concentration were found to significantly increase the incidence risk of COPD (Park et al., 2025). Furthermore, the distribution of this environmental exposure was shown to be socially unequal. The increased COPD risk attributable to air pollution was considerably more pronounced among residents of socioeconomically disadvantaged neighborhoods and among ethnic minority populations, including African American and Latino communities (Park et al., 2025).

In addition to respiratory effects, outdoor CO and NO_2 pollution has been shown to exert detrimental effects on the nervous system. A recent meta-analysis demonstrated that chronic exposure to elevated environmental NO_2 concentrations significantly increased both epilepsy incidence and seizure risk (Aljafen et al., 2025). High concentrations of traffic-related NO_2 are believed to increase seizure susceptibility by disrupting the blood-brain barrier and triggering neuroinflammatory processes within the central nervous system (Aljafen et al., 2025). The same analysis also reported a positive association between exposure to elevated ambient CO concentrations and epilepsy-related hospital admissions; however, this relationship was statistically weaker than that observed for NO_2 exposure (Aljafen et al., 2025).

The adverse effects of outdoor CO and NO_2 pollution extend beyond the respiratory and neurological systems and may also contribute to systemic and metabolic disorders. A long-term cohort study involving more than 60,000 participants in Taiwan found that prolonged exposure to environmental NO_2 and CO significantly increased the incidence of Non-Alcoholic Fatty Liver Disease (NAFLD), regardless of individual alcohol consumption habits (Chen et al., 2025). Compared with areas characterized by lower pollutant concentrations, individuals living in regions simultaneously exposed to elevated $PM_{2.5}$ levels and high ambient NO_2 or CO concentrations exhibited substantially greater risks of developing NAFLD (Chen et al., 2025). These findings strongly emphasize the synergistic effects of gaseous and particulate air pollutants on human metabolic health and underline the cumulative burden of environmental pollution on physiological systems (Chen et al., 2025).

2. MATERIALS AND METHODS

2.1. Emission Measurement Method

For emission measurements, a TESTO 340 flue gas analyzer available at the Central Research Laboratory of our university was utilized. The analyzer operates based on the electrochemical fuel cell principle. Any gaseous pollutant that can be electrochemically oxidized or reduced can be detected and quantified by the corresponding fuel cell integrated into the analyzer (Url, 2).

Electrochemical fuel cells are battery systems that operate using gases drawn from the ambient environment and introduced into the cell, where they serve as fuel. The primary application of fuel cells has traditionally been the generation of electricity from hydrogen fuel in spacecraft. In addition to consuming fuel gases, these cells also utilize oxygen during operation. Fuel cells are capable of functioning at very low gas concentrations, typically in the parts-per-million (ppm) range. The

absorption of gases into the cell and the resulting electrical output are regulated by a diffusion barrier within the cell. In most cases, the oxidation of the target gas results in electron transfer reactions, leading to a negative charge accumulation at the sensing electrode (Url, 2). The reactions occurring within the fuel cells are presented in Equations (1)-(6).

$$CO + H_2O \rightarrow CO_2 + 2H^+ + 2e^- \quad \textbf{(1)}$$

$$H_2S + 4H_2O \rightarrow H_2SO_2 + 8H^+ + 8e^- \quad \textbf{(2)}$$

Simultaneously, the reduction of oxygen occurs at the counter electrode:

$$O_2 + 2H^+ + 2e^- \rightarrow 2H_2O \quad \textbf{(3)}$$

In certain cases, the sensing electrode becomes positively charged as a result of reduction reactions involving the target gas.

Examples include:

$$NO_2 + 2H^+ + 2e^- \rightarrow NO + H_2O \quad \textbf{(4)}$$

$$Cl_2 + 2H^+ + 2e^- \rightarrow 2HCl \quad \textbf{(5)}$$

Under these conditions, oxygen is generated at the counter electrode through the oxidation of water:

$$2H_2O \rightarrow O_2 + 2H^+ + 2e^- \quad \textbf{(6)}$$

The electrical current (μA) generated as a result of the above electrochemical reactions is linearly proportional to the concentration of the measured gas. Since the current produced by electrochemical fuel cell sensors is derived from external gases rather than from the internal chemical resources of the cell, as is the case with conventional batteries, their operational lifetime is considerably longer. Under normal operating conditions, the service life of these sensors can reach approximately 3 to 4 years (Url, 2).

2.2. Air Quality Modeling Program

The emission data obtained from field measurements were entered into the AERMOD air quality dispersion modeling program together with the corresponding meteorological data. For this purpose, dispersion modeling was conducted for carbon monoxide (CO) and nitrogen dioxide (NO_2), for which limit values are specified in the Regulation on the Control of Industrial Air Pollution published by the Turkish Ministry of Environment, Urbanization and Climate Change. Since the combustion of natural gas does not result in significant sulfur dioxide (SO_2) or particulate matter emissions, no modeling studies were performed for these parameters.

Originally developed in 1991, the AERMOD model was officially adopted by the United States Environmental Protection Agency (EPA) in 2005. AERMOD is a steady-state atmospheric dispersion

model designed to assess the short-range dispersion of emissions from industrial facilities, typically within a maximum distance of 50 km from the source.

To estimate pollutant concentrations, AERMOD requires both emission data and meteorological input data. The AERMOD atmospheric dispersion modeling system consists of three main modules:

- AERMAP, a terrain preprocessor whose primary function is to establish the physical relationship between air pollution behavior and terrain characteristics. It generates receptor-specific geographic coordinates and elevation data.
- AERMET, a meteorological preprocessor that processes surface meteorological data, upper-air observations, and, when available, on-site meteorological tower measurements. It calculates atmospheric parameters required for dispersion modeling, including atmospheric turbulence characteristics, friction velocity, and mixing heights.
- The model input file, which contains emission source information and the associated source characteristics.

The AERMOD model applies a non-Gaussian probability density function under unstable atmospheric conditions and a Gaussian distribution under stable atmospheric conditions. For urban applications, the model incorporates the urban heat island concept. Furthermore, AERMOD provides more reliable predictions in areas characterized by complex terrain. Surface roughness length is a particularly influential parameter affecting concentration estimates. Previous studies have demonstrated that AERMOD exhibits high sensitivity to wind speed, wind direction, and surface roughness length.

The main capabilities of the AERMOD model include:

- Simulation of pollutant dispersion within distances of up to 50 km from the emission source,
- Application to complex industrial emission configurations, including single-point, multiple-point, area, line, and volume sources,
- Estimation of pollutant concentrations using both constant and variable emission rates, including gaseous and particulate deposition, as well as wet and dry deposition processes,
- Prediction of pollutant concentrations in both rural and urban environments.

The technical characteristics of the AERMOD program are presented in Table 1 (Erdoğan, 2012).

Table 1. Characteristics of the AERMOD Modeling System

Characteristic	AERMOD
Meteorological dataset	Surface-level meteorological data and upper-air sounding data
Meteorological profile	Generates vertical profiles for wind speed, temperature, and atmospheric turbulence
Emission dispersion	Gaussian distribution under stable atmospheric conditions; non-Gaussian probability density function under unstable atmospheric conditions
Rural/urban classification	Different urban conditions can be modeled through the inclusion of regional population data
Surface characteristics of the study area	Incorporates surrounding land surface characteristics, including surface roughness length, albedo, and Bowen ratio

The minimum meteorological data required for AERMOD simulations are presented in Table 2.

Table 2. Surface and Upper-Air Meteorological Data Required for AERMOD

Surface Meteorological Data for AERMOD	Upper-Air Meteorological Data for AERMOD
Wind speed (hourly)	Atmospheric pressure (00:00 and 12:00 GMT)
Wind direction (hourly)	Altitude (00:00 and 12:00 GMT)
Temperature (hourly)	Temperature (00:00 and 12:00 GMT)
Cloud cover (hourly)	Relative humidity (00:00 and 12:00 GMT)
Cloud base height (hourly)	Wind speed and direction (00:00 and 12:00 GMT)

The AERMOD model considers terrain characteristics and assumes that emitted pollutants move in accordance with the topographical structure of the study area. The model is based on the principle of pollutant conservation and does not explicitly account for chemical interactions among pollutants or their atmospheric transformation processes.

Under stable atmospheric conditions, AERMOD employs the Gaussian dispersion equation for both horizontal and vertical pollutant dispersion. Under unstable atmospheric conditions, the model utilizes a non-Gaussian probability density function to represent vertical dispersion.

AERMOD performs calculations based on the atmospheric surface boundary layer concept. In determining atmospheric stability, the model considers both the surface roughness length and the

Monin-Obukhov length (L). The relationship between surface roughness length, Monin-Obukhov length, and Pasquill-Gifford atmospheric stability classes is presented in Table 3.

Table 3. Atmospheric Stability Class Determination in AERMOD

Surface Roughness Length (m)	~L (m)	Pasquill-Gifford Stability Class
0.1	-12.5	A
0.1	-25	B
0.1	-65	C
0.1	--	D
0.1	+65	E
0.1	+30	F
0.5	-16	A
0.5	-50	B
0.5	-100	C
0.5	--	D
0.5	+100	E
0.5	+50	F

3. RESULTS

3.1. Boilers, Study Area, and Emission Measurement Campaign

Within the scope of the project, measurements were conducted to determine the combustion efficiency and flue gas emissions (CO, NO_x, and SO_2) of the boilers operating on the university campus. The characteristics of the boilers and flue stacks investigated in this study are presented in Table 4, while the spatial distribution of the boilers is illustrated in Figure 1.

Figure 1. Location of the boilers

The campus heating plant, which represents the most significant emission source on campus, was selected as the central reference point for defining the study area. According to the Regulation on the Control of Industrial Air Pollution, the impact area of an emission source is defined as a radius extending up to 50 times the stack height. Considering a stack height of 10 m for the heating plant chimneys, the corresponding impact area would be a radius of 500 m. However, to evaluate the effects of emissions over a broader region and to ensure that the influence zones of all sources remained within the selected study area, the modeling domain was expanded to 4 km × 4 km. A receptor grid was established by placing one receptor at 200 m intervals throughout the study area.

The study domain, emission source locations, and receptor grid configuration are presented in Figure 2. A total of 441 receptors were used to estimate ground-level pollutant concentrations at a receptor height of 1.5 m.

Figure 2. Distribution of emission sources and receptors within the 4 km × 4 km study area

Emission measurements and flue gas velocity determinations were carried out on 8 March 2024 for all boilers located on campus. Based on the measured data, pollutant mass emission rates (g s^{-1}) were calculated for each stack. The emission data used as model inputs are provided in Table 5.

Since natural gas was utilized as the fuel in all boilers, no SO_2 emissions were detected in the flue gases. Consequently, dispersion modeling was not performed for SO_2. Measurements identified the presence of CO and NO_x emissions in the flue gases. For modeling purposes, NO_x emissions were converted and expressed as NO_2 equivalents, and dispersion simulations were subsequently conducted for both CO and NO_2.

Table 4. Locations and Characteristics of the Boilers

Boiler Code	Boiler Location	Fuel Type	Served Facility	Boiler Capacity (kcal h^{-1})	Latitude	Longitude
K1	Central Heating Plant	Natural Gas	Blocks E-F	1,500,000	40°11'24.71"N	29°57'56.92"E
K2	Central Heating Plant	Natural Gas	Blocks C-D	2,500,000	40°11'24.71"N	29°57'56.92"E
K3	Central Heating Plant	Natural Gas	Blocks A-B	1,750,000	40°11'24.71"N	29°57'56.92"E
K4	H Block	Natural Gas	H Block	3,000,000	40°11'26.88"N	29°57'52.23"E
K5	TOBB Laboratory	Natural Gas	TOBB Laboratory	1,250,000	40°11'22.65"N	29°57'51.19"E
K6	Rectorate Building	Natural Gas	Rectorate Building	1,250,000	40°11'18.68"N	29°58'09.00"E
K7	Rectorate Building	Natural Gas	Library	1,350,000	40°11'18.68"N	29°58'09.00"E
K8	Lower Campus Entrance	Natural Gas	Vocational School and Prefabricated Buildings	5,750,000	40°11'32.10"N	29°58'02.01"E

Table 5. Emission Data Used as Model Inputs

Source No.	Source	Elevation (m)	NO_2 Emission (g s^{-1})	CO Emission (g s^{-1})	Stack Height (m)	Stack Gas Temperature (K)	Gas Velocity (m s^{-1})	Stack Diameter (m)
1	K1-K2-K3	571.21	0.155	0.097	10.0	465.7	5.2	0.60
2	K4	573.25	0.389	1.211	16.5	327.9	9.2	0.60
3	K5	584.72	0.081	0.028	10.0	334.9	5.5	0.60
4	K6-K7	576.96	0.083	0.047	11.5	382.4	3.9	0.60
5	K8	562.88	0.155	0.097	10.0	465.7	5.2	0.60

The major source of emissions at our university is the central heating plant serving Blocks A, B, C, D, E, and F. This facility contains the boilers designated as K1, K2, and K3. Since the boiler stacks are located adjacent to one another, the emission rates of each pollutant from these stacks were aggregated, and the heating plant was introduced into the dispersion model as a single emission source.

The H Block heating plant (K4) consists of three identical boilers. However, as only one boiler was operating during the measurement campaign, the measured emission values were multiplied by three and entered into the model as representative of all three units.

The coal-fired boilers located at the campus lower entrance and designated as K8 were decommissioned during the study period, while the transition to natural gas fuel was still ongoing. Therefore, the K8 heating plant was assumed to be equivalent to the central heating plant containing sources K1, K2, and K3. Emission source data from the central heating plant were used and incorporated into the model scenarios for K8.

For all measurements, the boilers were operated at maximum load in order to determine the highest possible emission levels and thereby represent worst-case emission conditions.

Sources K6 and K7 provide heating for the Rectorate and Library buildings, respectively. Since the K7 boiler serving the Library building was under maintenance during the measurement period, no measurements could be conducted for this unit. As the buildings and boilers are approximately equivalent in terms of capacity and characteristics, emissions measured from the K6 boiler were multiplied by two and entered into the model as a single source.

The average combustion efficiencies determined for the boilers are presented in Table 6.

Table 6. Average Combustion Efficiencies Determined for the Boilers

Boiler Code	Average Combustion Efficiency (%)
K1	94.2
K2	94.8
K3	87.1
K4	98.5
K5	97.9
K6	95.0

Overall, it can be observed that the combustion efficiencies of all boilers, with the exception of K3, exceed 94%. In contrast, the efficiency of boiler K3 was found to be approximately 87%. Accordingly, maintenance activities and a review of the excess air settings are recommended in order to improve the operational performance of this boiler.

3.2. Meteorological Data

The surface meteorological data used in the dispersion modeling study were obtained from the Bursa Osmangazi Meteorological Station (Station No. 17116), which is the nearest meteorological station to the university campus. Upper-air meteorological data were obtained from the Kadıköy Göztepe Pier Station (Station No. 17062) and processed using the AERMET preprocessor. The locations of the campus and the Bursa Osmangazi Meteorological Station are shown in **Figure 4**. The horizontal distance between the station and the campus is approximately 81 km.

The meteorological dataset consisted of hourly observations including temperature, atmospheric pressure, relative humidity, wind speed and wind direction, cloud cover, cloud base height, precipitation amount, and solar radiation. Wind roses provide information on the prevailing wind direction (i.e., the direction from which the wind originates) and wind speed distributions. The annual wind rose representing the study area for the year 2011 was generated using the BREEZE MetView software and is presented in **Figure 3**. Wind speeds were classified into specific velocity intervals, and the frequency of occurrence within each class was expressed as a percentage. Table 7 presents the wind speed classes and the frequency of winds by direction, based on data collected from the Bursa Osmangazi Meteorological Station for the year 2011. As shown in Table 7, northerly and easterly winds are the dominant wind directions in the study area.

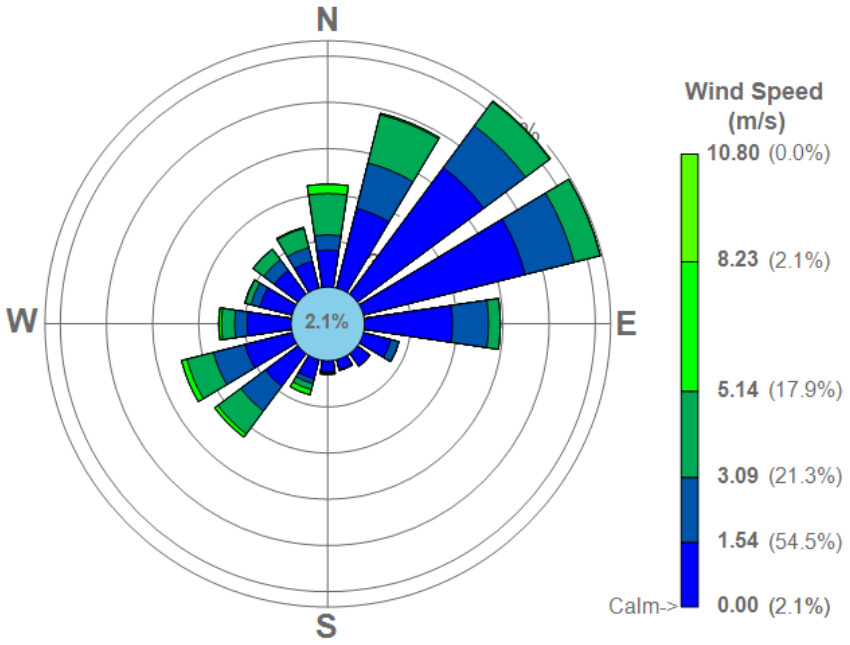

Figure 3. Wind rose illustrating the prevailing wind directions (wind origin) and wind speed distribution.

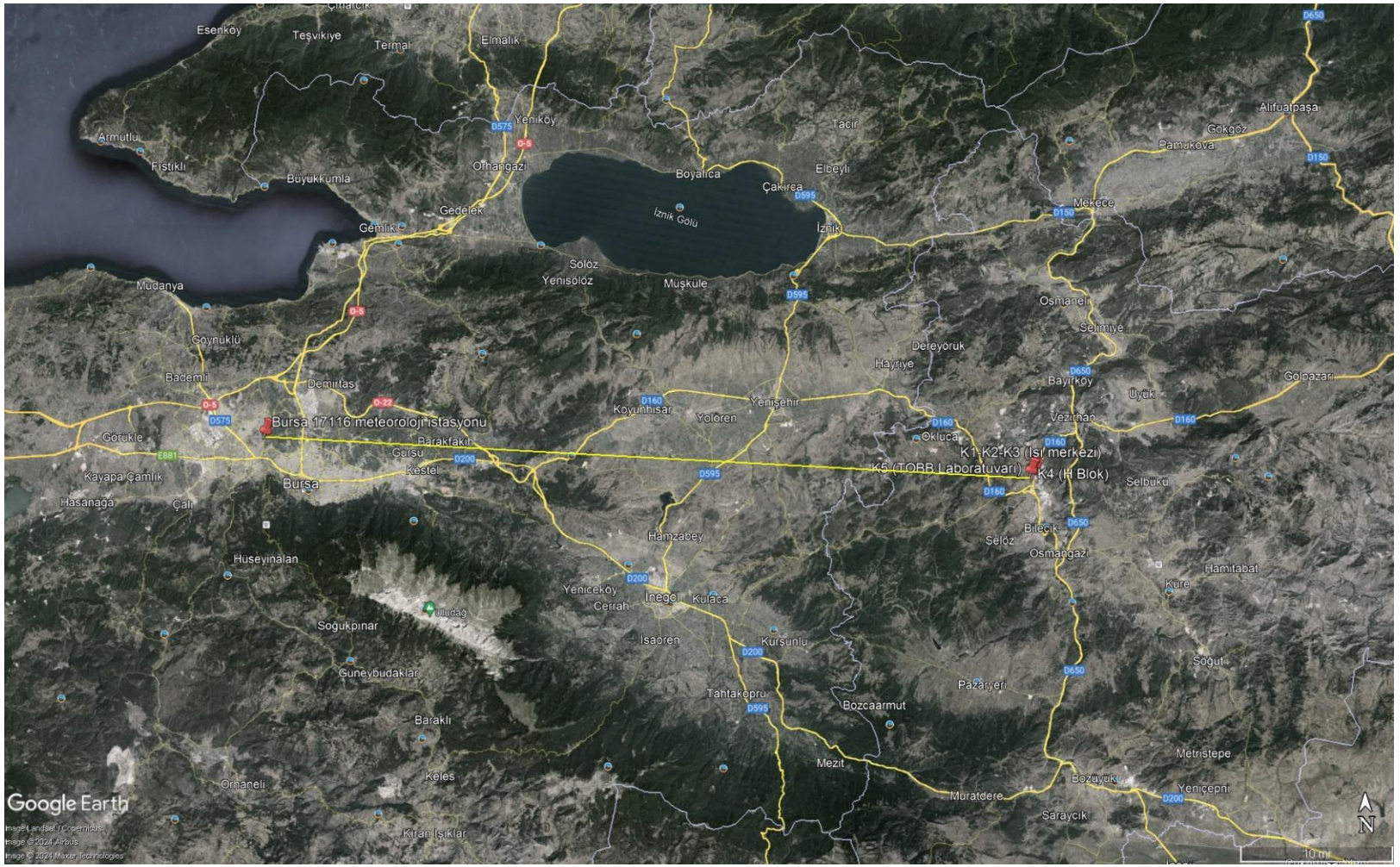

Figure 4. Location of the University Campus and the Bursa Osmangazi Meteorological Station on the map.

Table 7. Wind Speed Classes and Frequency of Occurrence by Wind Direction

Direction	Wind Speed Classes (m/s) ≤1.54	≤3.09	≤5.14	≤8.23	≤10.80	>10.80	Total Frequency Count	Frequency (%)
N	210	87	235	53	0	0	585	6.68
NNE	467	267	284	8	0	0	1,026	11.71
NE	896	297	171	5	0	0	1,369	15.63
ENE	949	288	153	1	0	0	1,391	15.88
E	500	206	67	0	0	0	773	8.82
ESE	160	46	1	0	0	0	208	2.36
SE	89	0	0	0	0	0	89	1.02
SSE	58	4	0	0	0	0	62	0.71
S	63	3	7	4	0	0	77	0.88
SSW	112	28	35	31	0	0	206	2.35
SW	231	176	162	23	0	0	592	6.76
WSW	276	185	156	32	0	0	649	7.41
W	250	71	75	14	1	0	411	4.69
WNW	188	53	34	2	0	0	278	3.16
NW	169	75	75	1	0	0	321	3.65
NNW	157	80	113	6	0	0	356	4.06

Additional Parameters	Value
Calm Conditions	184 (2.10%)
Missing Data	186 (2.12%)
Total Observations	8,760 (100%)
Average Wind Speed	1.76 m/s

3.3. Topographical Data

Elevation data for the study area were obtained from the Shuttle Radar Topography Mission (SRTM) 90 m Digital Elevation Data dataset available through the Consortium for Spatial Information (CGIAR-CSI) website. The data were processed using the AERMAP terrain preprocessor to generate the base format required by the dispersion modeling system. The resulting terrain data were subsequently used as input to the AERMOD dispersion model.

Figure 5 presents the three-dimensional representation of the study area generated after processing the topographic map within the AERMOD modeling framework.

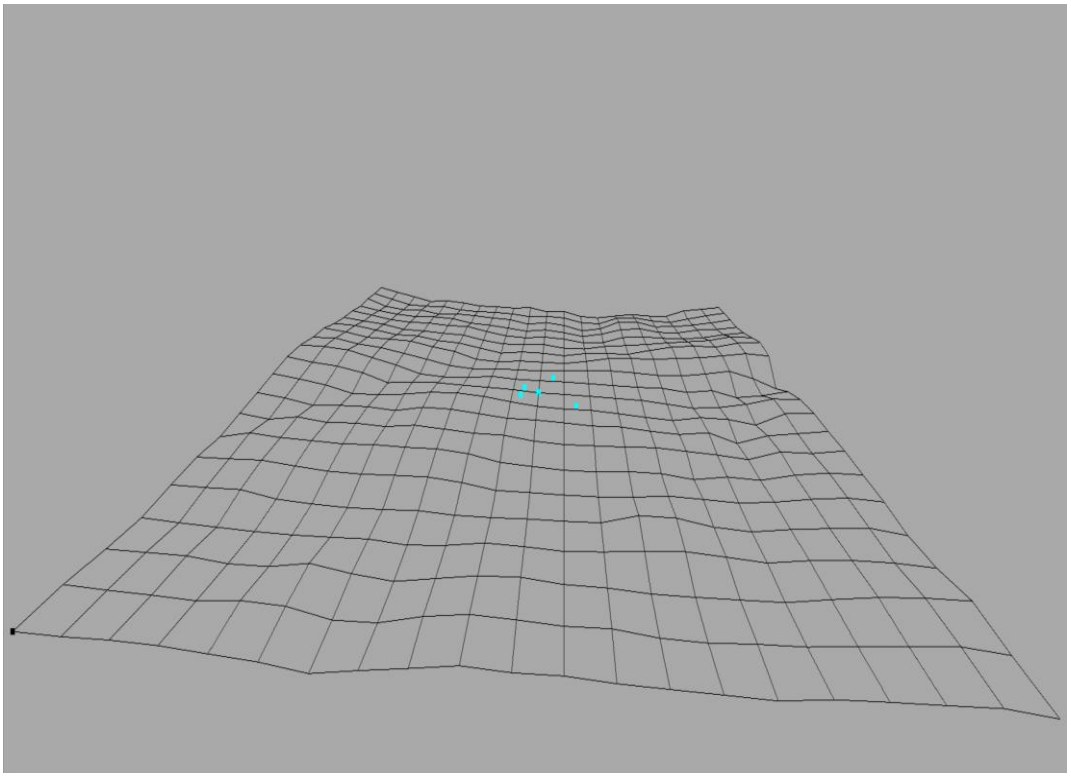

Figure 5. Three-dimensional representation of the study area obtained through processing of the topographic map using the AERMOD modeling system.

4. MODELING STUDY RESULTS

4.1. Applied Scenario

During the modeling study, all boilers operating within the university campus were assumed to be functioning at full capacity in order to assess air quality under the worst-case scenario. As natural gas is used as the primary fuel, particulate matter emissions from the flue gases were not expected. Furthermore, no SO_2 emissions were detected during flue gas measurements at any of the point sources.

Accordingly, dispersion modeling was conducted only for the pollutants detected in the stack emissions, namely CO and NO_2, and their concentration distributions were calculated.

4.2. Results Obtained for the NO_2 Parameter

Within the scope of the study, daily, monthly, and annual average concentrations of NO_2 were estimated for a one-year modeling period. The calculated values were compared with the Air Quality Contribution Values (AQCV) specified in Annex 2, Table 2.1 of the Regulation on the Control of Industrial Air Pollution. In addition, the calculated Short-Term Values (STVs) were compared with the corresponding Short-Term Limit Values (STLVs). The results are presented in Table 8.

As shown in Table 8, the calculated AQCV and STV values on daily, monthly, and annual bases are significantly below the applicable limit values. The contribution of the facility to ambient NO_2 concentrations remains below 1% of the relevant standards for all averaging periods.

The locations where maximum hourly, daily, monthly, and annual concentrations were observed, together with the corresponding concentration distribution simulations, are presented in Figure 6. Since residential heating activities in public institutions generally occur between 15 November and 15 March, monthly results are presented only for this five-month period.

Table 8. Air Quality Modeling Results for NO_2 and Comparison with Regulatory Limit Values

Period	AQCV (µg/m³)	UVS (µg/m³)	Contribution (%)	STV (µg/m³)	STLV (µg/m³)
January	0.496	200	0.248	2.780	40
February	0.455	200	0.228	2.075	40
March	0.334	200	0.167	1.500	40
November	0.468	200	0.234	2.129	40
December	0.435	200	0.218	1.431	40
Annual	0.425	200	0.213	1.720	40
Annual* (24-hour)	0.345	200	0.173	1.538	40

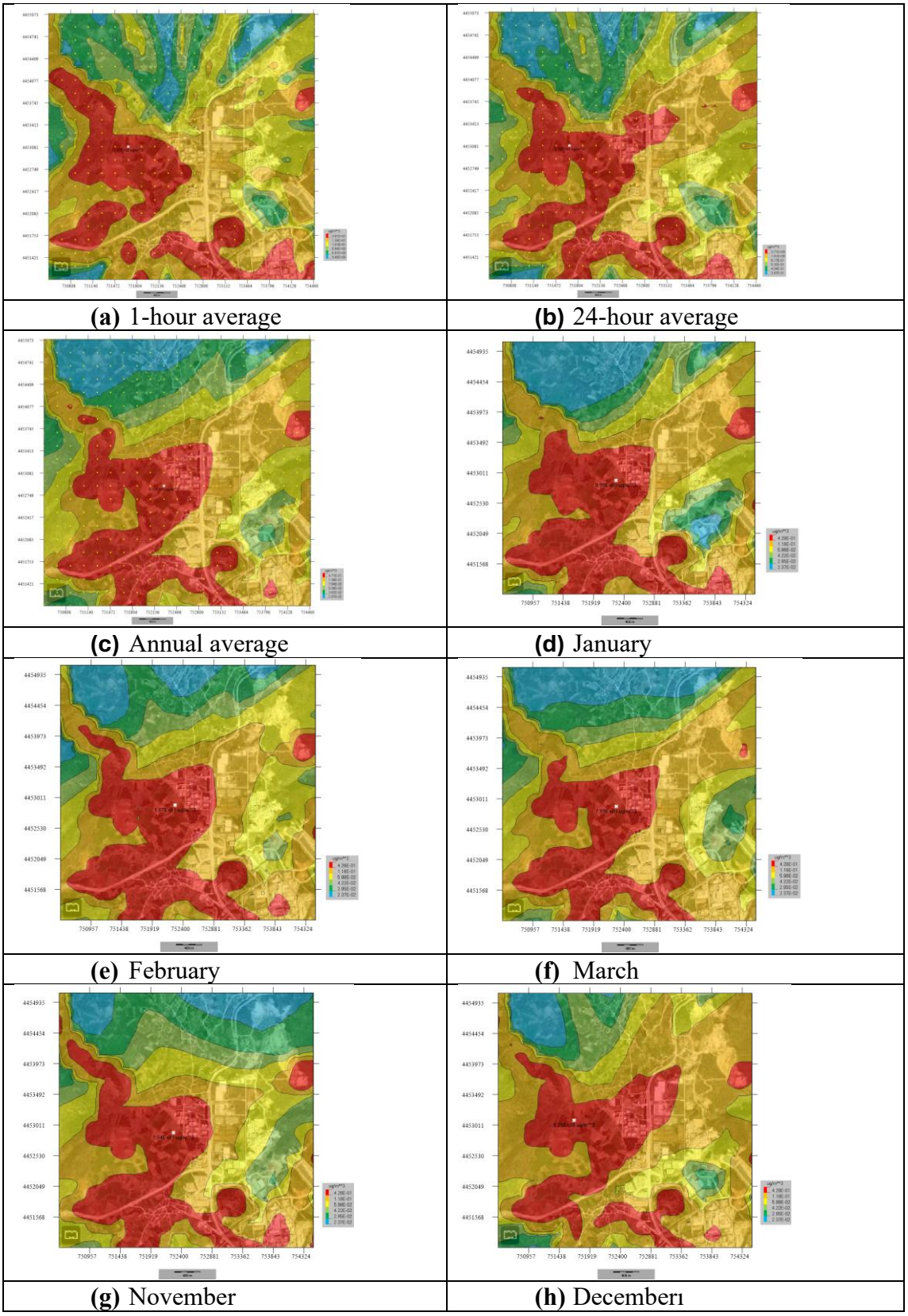

Figure 6. Locations of maximum NO_2 concentrations and concentration distributions within the impact area

The results indicate that daily, monthly, and annual AQCV values for NO_2 are substantially below the applicable UVS limits. Maximum concentrations were generally observed on the western side of the campus, while the highest concentration zone remained confined to the campus and its immediate surroundings.

4.3. Results Obtained for the CO Parameter

Within the one-year modeling period, daily, monthly, and annual average CO concentrations were estimated and compared with the Air Quality Contribution Values (AQCVs) specified in Annex 2, Table 2.1 of the Regulation on the Control of Industrial Air Pollution. The comparison is presented in Table 9. Since no corresponding short-term limit value exists for CO within the applicable regulation, the calculated STV values were not compared with a regulatory standard.

As shown in Table 9, AQCV values calculated on daily, monthly, and annual bases are well below the applicable limit values. The contribution of the facility to ambient CO concentrations remains below 8% of the relevant standards for all averaging periods.

The locations of maximum hourly, daily, monthly, and annual concentrations and their corresponding concentration distribution simulations are presented in Figure 7. As noted previously, monthly results are provided only for the heating season extending from 15 November to 15 March.

Table 9. Air Quality Modeling Results for CO and Comparison with Regulatory Limit Values

Period	AQCV (µg/m³)	UVS (mg/m³)	Contribution (%)	STV (µg/m³)	STLV
January	0.799	10	7.990	3.921	–
February	0.735	10	7.350	3.666	–
March	0.539	10	5.390	2.557	–
November	0.748	10	7.480	3.206	–
December	0.693	10	6.930	2.148	–
Annual	0.684	10	6.840	0.195	–

Period	AQCV (µg/m³)	UVS (mg/m³)	Contribution (%)	STV (µg/m³)	STLV
Annual* (24-hour)	0.556	10	5.560	2.374	–

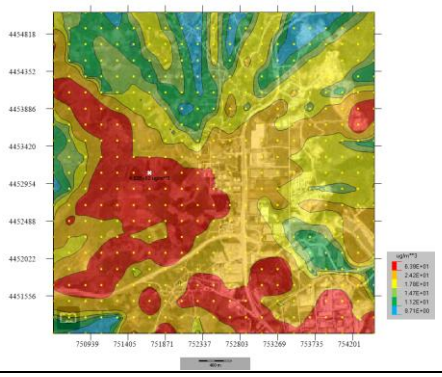

(a) 1-hour average

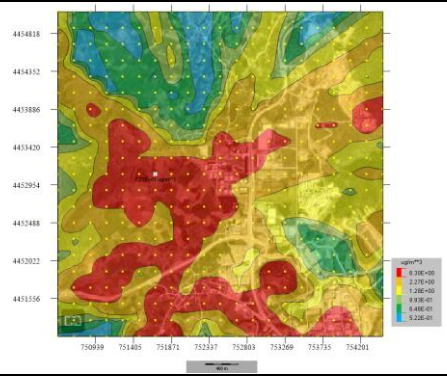

(b) 24-hour average

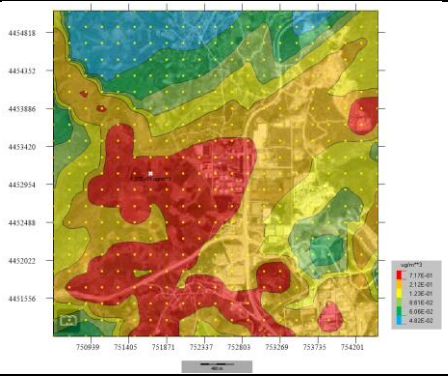

(c) annual average

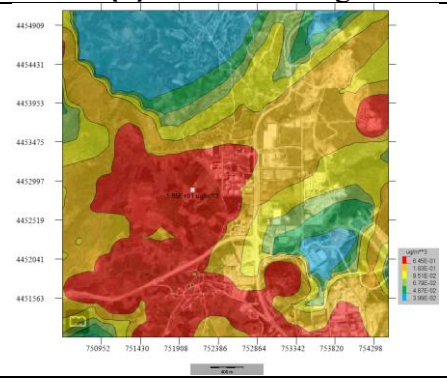

(d) January

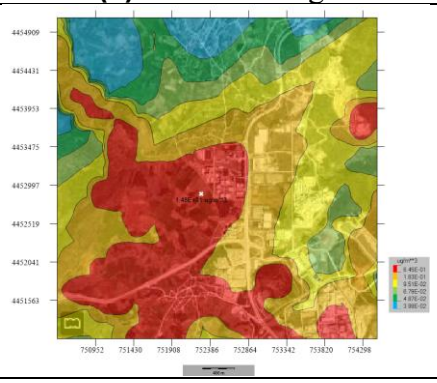

(e) February

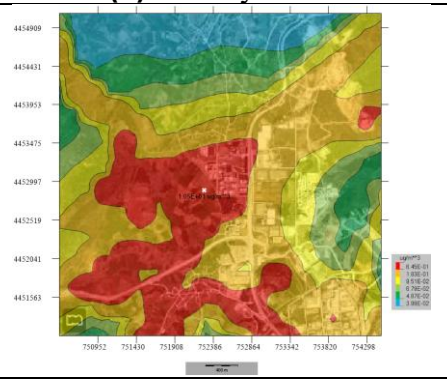

(f) March

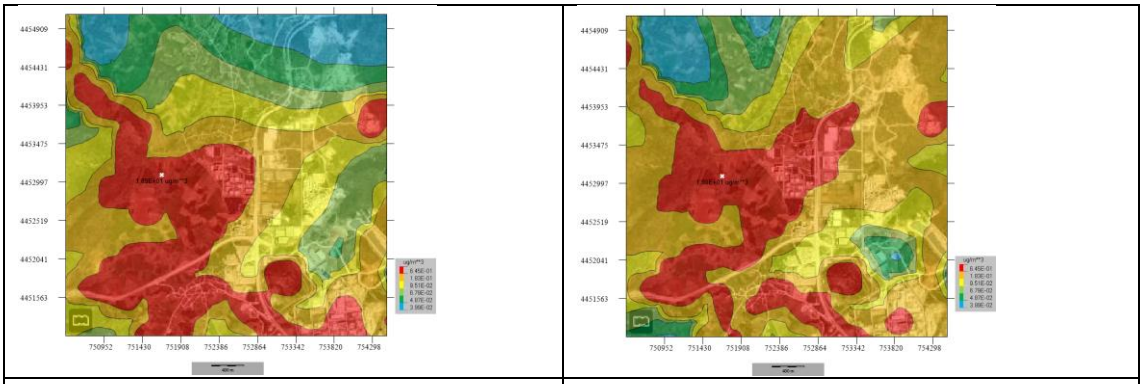

(g) November **(h)** December

Figure 7. Locations of maximum CO concentrations and concentration distributions within the impact area:

The results for CO are consistent with those obtained for NO_2. Daily, monthly, and annual AQCV values are substantially below the applicable regulatory thresholds. Maximum concentrations generally occur on the western side of the campus, while the area affected by elevated concentrations remains limited to the campus and its immediate vicinity.

5. CONCLUSIONS AND DISCUSSION

Air pollution resulting from heating activities is currently one of the most significant sources affecting urban atmospheric quality. This issue is particularly important in provinces such as Bilecik, where both urban traffic congestion and industrial activities contribute substantially to overall pollutant emissions. The combined influence of these sources may lead to considerable deterioration in air quality and consequently reduce the quality of life.

The present study aimed to assess the impact of fuel combustion for heating purposes on ambient air quality within the central campus of the university. During the project period, the replacement of coal-fired boilers with natural gas-fired units represented a significant improvement in terms of campus air quality.

Overall, the modeling results indicate that pollutant concentrations remain substantially below the applicable regulatory limits. Maximum concentrations were generally observed in the southwestern part of the campus as a result of prevailing wind patterns. When evaluated independently, the impact of campus heating sources on ambient air quality can be considered negligible. However, air quality should always be assessed comprehensively, and the cumulative impacts of surrounding facilities and emission sources should also be taken into account.

Evaluation of boiler combustion efficiencies revealed that all boilers except one achieved efficiencies exceeding 90%. These findings further emphasize the importance of regular

combustion gas analyses, efficiency assessments, timely maintenance, and operational adjustments to ensure optimal boiler performance and minimize environmental impacts.

REFERENCES

Aljafen, B. N., Shaikh, N., AlKhalifah, J. M., & Meo, S. A. (2025). Effect of environmental pollutants particulate matter (PM2.5, PM10), nitrogen dioxide (NO2), sulfur dioxide (SO2), carbon monoxide (CO) and ground level ozone (O3) on epilepsy. *BMC Neurology*, 25(133), 1-10.

An, R., & Yu, H. (2018). Impact of ambient fine particulate matter air pollution on health behaviors: a longitudinal study of university students in Beijing, China. Public health, 159, 107-115.

Bhat, M. A., Eraslan, F. N., Awad, A., Malkoç, S., Üzmez, Ö. Ö., Döğeroğlu, T., & Gaga, E. O. (2022). Investigation of indoor and outdoor air quality in a university campus during COVID-19 lock down period. *Building and Environment*, *219*, 109176.

Bostan, P., & Olcay, S. S. (2022). Dünden Bugüne Ülkemizde Yapılan Dış Ortam Havakirliliği Sağlık Etkileri Araştırmaları. *Türkiye Sağlık Araştırmaları Dergisi*, *3*(3), 22-29.

Chen, Y.-C., Pan, S.-C., Chin, W.-S., Wu, C.-D., & Guo, Y. L. (2025). Long-term exposure to ambient air pollution and the incidence of nonalcoholic fatty liver disease: a cohort study. *International Journal of Epidemiology*, 54(4), dyaf101.

Cichowicz, R., & Dobrzański, M. (2022). 3D spatial dispersion of particulate matter and gaseous pollutants on a university campus in the center of an urban agglomeration. *Energy*, *259*, 125009.

D'Amico, F., Lo Feudo, T., Gulli, D., Ammoscato, I., De Pino, M., Malacaria, L., Sinopoli, S., De Benedetto, G., & Calidonna, C. R. (2025). Investigation of Carbon Monoxide, Carbon Dioxide, and Methane Source Variability at the WMO/GAW Station of Lamezia Terme (Calabria, Southern Italy) Using the Ratio of Ozone to Nitrogen Oxides as a Proximity Indicator. *Atmosphere*, 16(251), 1-41.

Daxini, K., Turakhia, T., Iyer, R., & Chhabra, A. (2020, December). Assessment of ambient air quality of a college campus. In *2020 IEEE India Geoscience and Remote Sensing Symposium (InGARSS)* (pp. 193-196). IEEE.

Erdoğan, E.;2012, Sanayi Kaynaklı Hava Kirliliğinde Modellerin Kullanımının Karar Verme Sürecindeki Rolü, İTÜ Fen Bilimleri Enstitüsü Yüksek Lisans Tezi.

Liu, J., Cai, W., Zhu, S., & Dai, F. (2020). Impacts of vehicle emission from a major road on spatiotemporal variations of neighborhood particulate pollution—a case study in a university campus. *Sustainable Cities and Society*, *53*, 101917.

Park, S. L., Lichtensztajn, D., Yang, J., Wu, J., Shariff-Marco, S., Stram, D. O., Inamdar, P., Fruin, S., Larson, T., Tseng, C., Setiawan, V. W., Gomez, S. L., Samet, J., Le Marchand, L., Wilkens, L. R., Ritz, B., Wu, A. H., & Cheng, I. (2025). Ambient Air Pollution and Chronic Obstructive Pulmonary Disease: The Multiethnic Cohort Study. *Annals of the American Thoracic Society*, 22(5), 698-706.

Popescu, R. Ş., & Popescu, L. L. (2017). Assessment of air pollution, by the urban traffic, in university campus of bucharest. *Journal of Environmental Protection*, *8*(8), 884-897.

Sun, L., Héroux, M.-È., Xu, X., & Wheeler, A. J. (2025). Associations between residential fossil fuel combustion and indoor concentrations of nitrogen dioxide, carbon monoxide, and aldehydes in Canadian homes. *Journal of Exposure Science & Environmental Epidemiology*, 35, 649-660.

Szatyłowicz, E., Edizsoy, G., Öztürk, O., Yanaşık, İ., Siemiończyk, E., Skoczko, I., & Tabor, A. (2023). Pm10 ve Pm2 ile Hava Kirliliği Ölçüm Konsantrasyonunun Çok Boyutlu Analizi. 5 Bialystok Teknoloji Üniversitesi Kampüsünde. *Bilim ve Teknolojideki Gelişmeler*. *Araştırma Dergisi* , *17* (3).

(Url,1) Bursa'da Hava Kirliliğinin Ana Sebeplerinin Ortaya Konması ve Çözüm Önerilerinin Belirlenmesi.
https://www.bursa.bel.tr/dosyalar/birimek/210414091109_BuYuKsEHiR-HAVA-PROJESi-SON.pdf(Erişim tarihi 14/10/2022).

(Url,2) http://www.crowcon.com/talking_gas_electrochemical_systems.htm